Published in final edited form as:
J Immunol. 2008 April 15; 180(8): 5352–5359.

Inter-Strain Tissue-Infiltrating T Cell Responses to Minor Histocompatibility Antigens Involved in Graft-Versus-Host Disease as Determined by V*β* Spectratype Analysis[1]

Jenny Zilberberg, **Danielle McElhaugh**[2], **Loise N. Gichuru**, **Robert Korngold**[3], and **Thea M. Friedman**
The Cancer Center, Hackensack University Medical Center, Hackensack, NJ 07601

Abstract

Lethal graft-vs-host disease (GVHD) can be induced between MHC-matched murine strains expressing multiple minor histocompatibility Ag differences. In the B6–>BALB.B model, both $CD4^+$ and $CD8^+$ donor T cells can mediate lethal GVHD, whereas in the B6–>CXB-2 model, only $CD8^+$ T cells are lethal. TCR V*β* CDR3-size spectratyping was previously used to analyze $CD8^+$ and $CD4^+$ T cell responses in lethally irradiated BALB.B and CXB-2 recipients, which showed significant overlap in the reacting repertoires. However, $CD4^+$ T cells exhibited unique skewing of the V*β*2 and 11 families in only BALB.B recipients. These V*β* family reactivities were confirmed by immunohistochemical staining of lingual epithelial infiltrates, and by positive and negative selection V*β* family transfer experiments for GVHD induction in BALB.B recipients. We have now extended these studies to examine the T cell repertoire responses involved in target tissue damage. Infiltrating B6 host-presensitized $CD8^+$ and $CD4^+$ T cells were isolated 8–10 days post-transplant from the spleens, intestines and livers of CXB-2 and BALB.B transplant recipients. For both T cell subsets, the results indicated overlapping tissue skewings between the recipients, also between the tissues sampled within the respective recipients as well as tissue specific responses unique to both the BALB.B and CXB-2 infiltrates. Most notably, the $CD4^+V\beta\ 11^+$ family was skewed in the intestines of BALB.B but not CXB-2 recipients. Taken together, these data suggest that there are likely to be target tissue-related anti-multiple minor histocompatibility Ag-specific responses in each of the strain recipients, which may also differ from those found in peripheral lymphoid organs.

Immunotherapeutic strategies have continued to gain recognition as viable alternatives to more conventional modalities for the treatment of cancer. In this regard, adoptive T cell therapy through allogeneic blood and marrow transplantation (BMT)[4] has been widely used for its anti-tumor effects against hematological malignancies (1). However, donor T cell-mediated graft-vs-host disease (GVHD) continues to be the principal complication of allogeneic BMT, along with graft rejection, leukemic relapse, and opportunistic infections (2,3). The depletion of T cells from donor stem cell inocula, while significantly reducing the development of GVHD, has been clearly associated with increased incidence of the other risk factors, probably due to the slow pace of immunological reconstitution in the recipients (4). Thus, the key to

[1]This work was supported in part by the National Institutes of Health Grants R01 HL55593 and R01 HL75622.

3Address correspondence and reprint requests to Dr. Robert Korngold, Cancer Center, Hackensack University Medical Center, Jurist Research Building, Room 356, 30 Prospect Avenue, Hackensack, NJ 07601. E-mail address: rkorngold@humed.com.
[2]Current address: Merck Research Laboratories, West Point, PA 19486.

Disclosures
The authors have no financial conflict of interest.

[4]Abbreviations used in this paper: BMT, blood and marrow transplantation; GVHD, graft-versus-host disease; GVL, graft-vs-leukemia; miHA, minor histocompatibility Ag; TDL, thoracic duct lymphocytes.

successful allogeneic BMT lies in the ability to ameliorate GVHD while still enabling the beneficial donor T cell effects of graft-vs-leukemia (GVL) responses, enhanced stem cell engraftment, and the capacity to resist infections.

An approach we have previously used as a diagnostic tool for evaluating both GVHD and GVL cellular responses is TCR Vβ CDR3-size spectratype analysis (5,6). This analysis facilitates the characterization of specific alloreactive or leukemia-reactive clonal or oligoclonal T cells. To this end, spectratyping was used to analyze the $CD8^+$ and $CD4^+$ donor T cell responses involved in the generation of GVHD across the MHC $H2^b$-matched, minor histocompatibility Ag (miHA)-mismatched mouse transplantation models, B6->C.B10-$H2^b$ (BALB.B) and B6 –>CXB-2, a recombinant inbred strain. Spectratype analysis of the reacting $CD8^+$ and $CD4^+$ T cells indicated overlapping skewing of several Vβ families in both the BALB.B and CXB-2 recipients, and specifically unique skewing of the $CD4^+$Vβ2 and 11 families in the BALB.B recipients (7). In addition, immunohistochemical staining of lingual epithelial tissue from BALB.B recipients of naive B6 $CD4^+$ T cells also correlated with the involvement of several of the spectratype-skewed Vβ families in GVHD lesions, and depletion of these Vβ families from the donor inoculum resulted in a significant increase in survival of the transplanted recipients (8,9). Conversely, transplantation of B6 $CD4^+$V$\beta2^+$ and 11^+ T cells into BALB.B recipients resulted in the development of severe lethal GVHD (9). The identification of reactive T cells to host alloantigens could then be potentially used as a means to direct the manipulation of the donor T cell inoculum in an effort ameliorate GVHD and permit GVL effects.

In this study, we have extended our analysis to examine the Vβ repertoire of the tissue-infiltrating B6 $CD4^+$ and $CD8^+$ T cells responding to miHA in lethally irradiated BALB.B recipients, to investigate the relevancy of the previously detected spectratype-skewed T cell families obtained from the thoracic duct lymphocyte (TDL) (7,8) and splenic populations (10) with regard to GVHD immunopathology in the major target organs of the liver and intestinal tract. The results indicated overlapping CDR3-size skewing between the B6 $CD8^+$ T cells in both the BALB.B and CXB-2 combinations. In addition, the B6 $CD4^+$ T cells also exhibited overlapping CDR3-size skewing between the BALB.B and CXB-2 recipients. Lastly, some T cell responses among the tissues of each recipient strain demonstrated overlapping size skewing, while, most notably, there were tissue-specific responses unique to each of the BALB.B and CXB-2 infiltrates.

Materials and Methods

Mice

C57BL/6J (B6), C.B10-$H2^b$/LiMedJ (BALB.B), and CXB-2/By (CXB-2) mice were purchased from, and/or raised in our breeding colony from breeder pairs provided by, The Jackson Laboratory. The eGFP transgenic mice, on a B6 background, were obtained from the laboratory of Dr. Jon Serody (University North Carolina, Chapel Hill, NC) and bred in our colony. Male donor and recipient mice between 8 and 12 wk of age were used in all experiments. Mice were kept in a pathogen-free environment in autoclaved microisolator cages and were provided with acidified (pH 2.5) water and autoclaved food ad libitum. The Hackensack University Medical Center's Institutional Animal Care and Use Committee approved all protocols in this study.

Preparation of donor cells

T cell-enriched donor cells were prepared from a pooled spleen and lymph node cell suspension (in 0.1% BSA in PBS) from B6 mice that were presensitized (1.5×10^7 cells; i.p. injection; 2 1/2-weeks apart) with either BALB.B or CXB-2 splenocytes. We have previously demonstrated that both naive and presensitized donor T Cells can mediated severe lethal GVHD

and exhibit the same skewing pattern (8,9). Cells were harvested (7–10 days after second injection) and initially resuspended in Gey's balance solution containing 0.7% NH_4Cl for RBC lysis and were passed through a 70-um cell strainer to remove dead cells. B cells were removed by panning the cell suspension on goat anti-mouse IgG-coated plastic petri dishes for 1 h at 4° C. The nonadherent (T cell-enriched) cells were harvested, and the resulting population was greater than 80% $CD3^+$, as determined by flow cytometry. To obtain $CD8^+$ T cells, $CD4^+$ cells were depleted by incubating the T cell-enriched population with RL172 mAb (1/100 dilution) and guinea pig C (1/20 dilution; Rockland) in a water bath at 37°C for 50 min. Similarly, $CD4^+$ T cells were obtained by incubating the T cell-enriched suspension with 3.168 mAb in the presence of C, to deplete the $CD8^+$ population. Enriched cell were >85% pure for the desired population, as determined by flow cytometry. Cells were washed two times and resuspended in PBS for i.v. injection.

To purify for a particular Vβ family, enriched eGFP $CD4^+$ T cells were labeled with the appropriate PE-conjugated anti- Vβ mAb (BD Pharmingen), followed by incubation with anti-PE microbeads (Miltenyi Biotec). Labeled cells were purified by AutoMACS positive selection (Miltenyi Biotec), yielding a purity of the selected cells of >90%.

GVHD induction

BALB.B and CXB-2 mice were exposed to lethal irradiation (9 Gy, split-dose) from a ^{137}Ce source (Gammacell 40 Exactor, MDS Nordion) and injected ~4 h later with 2×10^7 $CD8^+$ or $CD4^+$ enriched T cells from host-presensitized B6 mice. The onset of severe GVHD occurs between days 20–30 and mortality accumulates over the next 2 mo, usually reaching 100% by days 70–80 (7–9,11–13). Using immunohistochemistry, we have previously examined the infiltration of T cells into the GVHD target tissues, and have found T cells there as early as seven days post-transplant and increasing infiltration out to days 20–30, concomitant with developing epithelial target tissue injury (14).

Isolation of tissue-infiltrating mononuclear cells

Organs from five to seven mice were pooled together to harvest infiltrating T cells. Mice were euthanized by CO_2 inhalation and perfused by intra-cardiac injection of PBS. Subsequently, the liver, spleen, and the distal ileum of the intestinal tract were excised and placed in cold PBS for further processing. The livers were dissociated by passage through a stainless steel mesh and the dislodged tissue was collected and centrifuged at $750 \times g$ for 10 min at 4°C. The liver pellets were digested for 15 min at 37°C with 0.05% type II collagenase (Sigma-Aldrich) in Ca^{2+} and Mg^{2+} free HBSS containing 5% FCS. After two washes in 4°C HBSS, the digested pellet was resuspended in 5 ml of Ultraspec (Biotecx Laboratories) for subsequent RNA extraction. The spleens were ground, centrifuged at $300 \times g$ for 10 min, and resuspended in Ultraspec. Sections of the small intestine were flushed with PBS to remove the contents, cut into small pieces, and resuspended in HBSS-free containing 5% FCS and 0.1% 0.5 M EDTA. Dissociation of the infiltrating lymphocytes was performed by continuously shaking the samples at 37°C, for 20 min. This procedure was repeated two times; after each time, the supernatant containing the dissociated cells was collected and fresh solution was added to the remaining pieces of intestine. The collected solution was centrifuged at $300 \times g$ for 10 min and the pellet was resuspended in 5 ml of Ultraspec.

Immunopathology associated with infiltration of $CD4^+V\beta11$ T cells

To quantify tissue damage caused by the $CD4^+V\beta11^+$ family, unseparated $CD4^+$ (2×10^7 cells), or Vβ family-enriched BALB.B presensitized B6 eGFP $CD4^+$ T cells were injected into lethally irradiated BALB.B and CXB-2 recipients at a dose comparable to their relative number in the unseparated $CD4^+$ enriched T cells fraction (9). Evaluation focused on tissue sections (6 μm) from the small intestine, as one of the major target organs in these mouse strain combinations

(9,13). To preserve the eGFP, the tissue was fixed overnight in 4% paraformaldehyde, followed by a 24 h fixation in 10% sucrose before Tissue-Tec OCT compound embedding (15). Infiltration of cells was quantified as the number of $eGFP^+$ cells per field area ($pixel^2$) using ImageJ 1.38x software (National Institutes of Health, Bethesda, MD). Likewise, apoptosis of epithelial cells was determined using TUNEL staining (Apoptag detection kit, Chemicon, CA) according to the manufacturer's instructions. To determine tissue morphology, consecutive tissue sections to those used for counting infiltration were counterstained with Mayer H&E stain. Statistical significance of differences in infiltration and apoptosis in the tissues between BALB.B and CXB-2 recipient mice was determined using a Student's *t* test analysis on the mean count of three different fields of observation (10× magnification) from two separate mice each.

CDR3-size spectratype analysis

Total cellular RNA, RT-PCR, and CDR3-size spectratype analysis was performed as previously described (10). In brief, RNA was isolated by chloroform extraction followed by isopropanol precipitation. The poly(A) $^+$ portion of the total RNA was converted into cDNA using oligo(dT) as a primer for reverse transcription. Seminested PCR was performed by using a panel of Vβ sense oligoprimers (IDT technologies), and 2 Cβ antisense oligoprimers, the second Cβ being fluorescently labeled Applied Biosystems. PCR products were run on an ABI 3130 capillary gel system at the Molecular Resource Facility of University of Medicine and Dentistry of New Jersey. Analyses were performed using GeneMapper Software (version 3.7) from PE-Applied Biosystems.

Quantitation of CDR3-size usage

To determine the statistical significance of the spectratype data for each Vβ family, spectratype analysis was repeated 3× (three mice each) for normal B6 control $CD4^+$ and $CD8^+$ splenic T cells and 3× for each experimental group (three to five mice/group). The areas under the corresponding peaks representing varying CDR3 size lengths were averaged for each Vβ histogram. A CDR3-size length was considered skewed if the mean area under the peak was greater than the mean ± 3× SD of the corresponding control peak (10). Unique refers to a single peak within a particular Vβ family that it is skewed in one strain and/or tissue but not in the other. Peaks of the same PCR-size length in different Vβ families are independent of one another containing different CDR3 regions.

Results

T cell repertoire analysis in GVHD target tissue of BALB.B and CXB-2 recipient mice transplanted with host-presensitized B6 donor $CD8^+$ and $CD4^+$ T cells

Using TCR Vβ CDR3-size spectratype analysis of circulating TDL in BALB.B and CXB-2 mice transplanted with presensitized B6 $CD8^+$ or $CD4^+$ T cells, we previously demonstrated that both miHA-mismatched strain combinations share a limited set of unique, as well as, overlapping Vβ families involved in GVHD reactivity (7,8). Because tissue-specific expression of miHA can occur in both the hematopoietic compartment and the GVHD-target tissues (16, 17), corresponding differences might be reflected in the tissue-infiltrating T cell repertoire. Therefore, in the present study, we analyzed the Vβ repertoire of B6 $CD8^+$ and $CD4^+$ T cells responding to miHA in the BALB.B and CXB-2 GVHD-target tissues following transplantation to test this hypothesis. To this end, lethally irradiated BALB.B and CXB-2 recipients were transplanted with 2.0×10^7 host-presensitized B6 $CD8^+$ or $CD4^+$ T cells and spectratype analyses were performed on the donor T cells harvested from the spleens, livers and intestines of these mice on day 10. A representative spectratype for the $CD4^+$ V$\beta 11^+$ T cell family (Fig. 1) demonstrates the presence of overlapping and unique responses in the target

tissues of both recipient mice (i.e., the liver of CXB-2 mice presented a peak at length 164 not skewed in the BALB.B strain).

The results of the spectratype analyses of tissue-infiltrating B6 $CD8^+$ T cells in BALB.B and CXB-2 recipients are summarized in Table I. Overlapping tissue skewing (as defined by the presence of at least one overlapping CDR3-size length in a particular Vβ family) was found for Vβ7, 8.2, 14, 18, and 20 in the spleens, Vβ7, 8.1, 10, 14, 15, and 18 in the intestines and Vβ6, 7 and 14 in the livers in both strain combinations. Furthermore, the V$\beta14^+$ T cell family, which was previously found to be skewed in the TDL of transplanted BALB.B and CXB-2 recipients (7), was expanded in all the analyzed organs of both strains. Of most interest, two additional unique V$\beta14^+$ CDR3-size lengths (158 and 161) were skewed in the intestinal infiltrates of the BALB.B recipients.

Similarly, the spectratype analyses of tissue-infiltrating B6 $CD4^+$ T cells are summarized in Table II. There was overlapping tissue skewing in Vβ2, 9, 10, 11, and 13 in the spleens, Vβ2, 5, 9, and 10 in the intestines and Vβ2, 5, 9, 10, and 11 in the livers in both strain combinations. The spectratype data from this tissue study were then compared with the previously identified TCR Vβ use of $CD8^+$ and $CD4^+$ T cells in the TDL of transplanted BALB.B and CXB-2 recipients that were analyzed at day 5 post-transplant (7,8). A summary of this comparison, performed between resolvable Vβ families, is presented in Table III for $CD8^+$ T cells and in Table IV for $CD4^+$ T cells. The Vβ families 8.1, 8.2, and 8.3 were combined to directly compare the results of both sets of data.

In the BALB.B recipients, Vβ1, 4, 6, 8.1/.2/.3, 9, 10, 11, and 14 were skewed in both the $CD8^+$ TDL cells and at least one of the tissues analyzed, Vβ3, 5, 7, 13, 15, 16, and 20 were skewed in at least one organ, but not in the TDL (Table III). Vβ1, 6, 8.1/.2/.3, 10, 11, and 14, exhibited reactivity in both the $CD8^+$ TDL and in at least one of the analyzed tissues of CXB-2 recipient mice, whereas Vβ2, 3, 4, 7, 12, 13, 15, 16, and 20 were not skewed in the TDL, but were in one or more of the targeted organs. Finally, Vβ9 was skewed in the TDL and not reactive in the spleen, intestine or the liver (Table III).

In a similar manner, comparisons of the $CD4^+$ Vβ families demonstrated that in the BALB.B recipients Vβ2, 6, 7, 8.1/.2/.3, 9, 10, 11, and 13 were skewed in both the TDL and at least one of the GVHD target tissues, whereas Vβ5, 15, and 20 were skewed in at least one tissue, but not in the TDL (Table IV). In contrast, Vβ4 was skewed in the TDL, but not in any other organ. Likewise, in the CXB-2 mice, Vβ6, 7, 8.1/.2/.3, 9, 10, 12, 13, 14, 16, and 18 were skewed in the TDL and in at least one of the tissues analyzed, and Vβ2, 3, 5, 11, and 20 were skewed in a minimum of one organ, but not in the TDL. Vβ4 was again skewed in the TDL, but not in the tissues (Table IV).

The B6 $CD4^+$ Vβ2 and Vβ11 T cell families, which in previous studies were shown to cause lethal GVHD in BALB.B but not CXB-2 irradiated recipients (9), were expanded in the TDL, spleen, liver, and intestine of BALB.B mice (Table IV). These two Vβ families exhibited skewing in a unique CDR3-size length (167 and 158, respectively). Although Vβ2 and Vβ11 were not skewed in the TDL of CXB-2 recipients, Vβ2 was skewed in all three tissues analyzed and Vβ11 was only skewed in the liver and the spleen of the CXB-2 mice but not in the intestine (Table IV).

Vβ CDR3-size usage overlap between tissues

We have previously examined the sequence of the CDR3 regions in the alloreactive peaks from the $CD8^+V\beta14^+$ T cells in the BALB.B and CXB-2 recipients and determined that the sequence of the coincident peaks is identical (10) and unpublished data. Given that the CDR3 region of the TCR confers Ag specificity there is a high probability that these identical TCR β-chains

are responding to the same Ag. We therefore hypothesized that a commonly skewed CDR3-size length in a Vβ family that had infiltrated more than one tissue was associated with a particular miHA that was likely to be ubiquitously and highly expressed within the target organs. Although more definitive evidence to support this hypothesis would come from the analysis of miHA expression, for these two mouse models to date, no physiologically relevant miHA for eliciting severe and lethal GVHD have been identified. Thus, Tables V and VI summarize the distribution of skewed peaks for each Vβ family within the different tissues for the CD8 and CD4 T cell subsets, respectively. The results demonstrated that in the CD8 T cell subset, Vβ7, 8.1, 14, 16, and 20 and Vβ1, 7, 11, and 14 were skewed in the spleen, intestine and liver of BALB.B and CXB-2 recipients respectively. Vβ3, 8.2 15, and 18 in BALB.B recipients and Vβ2, 6, 8.2, 15, 16, and 20 in the CXB-2 mice exhibited skewing in at least two tissues (Table V). In the CD4 subset, Vβ2, 5, 8.3, 9, 10, and 11 in BALB.B recipients, and Vβ2, 7, 9, 10, 13, and 20 in the CXB-2 strain were skewed in all three organs (Table VI). Furthermore, Vβ6 and 13 in BALB.B recipients and Vβ5, 8.3, 11, and 18 in the CXB-2 mice exhibited skewing in two tissues.

In situ localization of tissue-infiltrating CD4$^+$Vβ11$^+$ T cells

We have previously determined that several CD4$^+$Vβ^+ families exhibited CDR3-size skewing, indicative of alloreactivity in the both the B6–>BALB.B and B6–>CXB-2 BMT models. However, only the CD4$^+$Vβ11$^+$ family resulted in severe lethal GVHD in the BALB.B recipients and CD4$^+$ T cells cannot mediate lethal GVHD in CXB-2 (9,12). To confirm that the CD4$^+$Vβ11$^+$ family was associated with GVHD immunopathology, fluorescence microscopy and TUNEL analysis were used to examine their involvement with in situ target tissue infiltration. Lethally irradiated BALB.B and CXB-2 recipient mice were injected with either 2×10^7 enriched eGFP CD4$^+$ or 4.6×10^5 (their frequency in the unseparated CD4$^+$ population) purified eGFP CD4$^+$Vβ11$^+$ B6 T cells. Spectratype analysis of tissue-infiltrating T cells also showed that this family was skewed in the intestines of BALB.B, but not CXB-2 mice (Table II); hence, we sought to quantify the damage associated with CD4$^+$Vβ11$^+$ infiltration in both strain combinations. Fig. 2, *A* and *B* are representative images of infiltrating B6 eGFP CD4$^+$Vβ11$^+$ T cells in BALB.B and CXB-2 recipients, respectively. Most notably, both infiltrating cells (Fig. 2*C*, $p \leq 0.01$) and TUNEL$^+$ (apoptotic) cells (Fig. 2*D*, $p \leq 0.02$) were significantly greater in BALB.B intestinal tissue compared with that of CXB-2 recipients.

Discussion

Previous studies conducted in our laboratory demonstrated that transplantation of H2^b-matched B6 anti-T cell depleted bone marrow and CD4$^+$ T cells into lethally irradiated BALB.B recipients can cause lethal GVHD, but failed to develop lethal disease in CXB-2 recipients (12). CXB-2 mice express a subset of the miHA found in BALB.B mice (18), and TCR Vβ CDR3-size spectratype analysis of TDL in transplanted mice from both strain combinations revealed the use of a limited set of overlapping Vβ families involved in GVHD reactivity, as well as some unique Vβ responses in BALB.B recipients (8). This result suggested the existence of a distinct set of miHA epitopes associated with CD4$^+$ responses in BALB.B recipients that might account for the increased severity of GVHD. Indeed, subsequent experiments indicated that deletion of the B6 Vβ2 and Vβ11 CD4$^+$ families from donor inoculum prevented severe GVHD development, and conversely, transplantation of only those two Vβ families could cause lethal GVHD (8). Several studies have indicated that miHA are tissue-restricted (16,17), and Rosset et al. also found a relationship between tissue-specific distribution of dominant miHA and specific organ destruction caused by GVHD (17). Although T cell spectratype analysis has previously been used to determine the reactive Vβ families involved in the generation of GVHD responses (6,7,19), the tissue-dependency of miHA expression suggests that the connection must be made between the presence of alloreactive T cells in the hematopoietic compartment

(where responses initiate) with those found in the GVHD-target tissues. Therefore, in the present study, we analyzed the Vβ repertoire of the tissue-infiltrating B6 $CD8^+$ and $CD4^+$ T cells responding to miHA in the BALB.B and CXB-2 strains to investigate this association. Noteworthy is the finding that for the skewed Vβ families of T cells infiltrating the GVHD-target tissues, in most cases (66% of all skewed $CD8^+$ and 73% of all skewed $CD4^+$ Vβ families), only a single CDR3-size peak was skewed, suggestive of a mono/oligoclonal expansion to a particular miHA. These results provide the necessary basis to further characterize the nature of tissue-specific alloresponses arising from a limited set of miHA.

The spectratype data obtained in this study were compared with previously identified TCR Vβ use of $CD4^+$ (8) and $CD8^+$ (7) TDL from BALB.B and CXB-2 mice transplanted with host-presensitized B6 T cells, and analyzed at day 5 post-transplant (Tables III and IV). This comparison revealed several differences between the skewing patterns of TDL and those of tissue-infiltrating lymphocytes. One explanation for this observation, as we previously demonstrated, is that the alloreactive T cell repertoire can change during the development of GVHD (10). Some Vβ families were transiently skewed over time, most were consistently skewed throughout the progression of the disease, and other Vβ families did not exhibit any skewing until later in the development of disease. Because the evaluation of the TDL was at day 5 post-transplant and the spectratype analysis of tissue-infiltrating lymphocytes was done between days 8–10, it is likely that Vβ families with a later onset of reactivity were not skewed in the TDL studies, and other families that were initially skewed but not consistent over time may precipitate the initial tissue damage leading to the expression of additional Ags, but then no longer continue to receive the necessary stimulation once they cause damage to the target tissues (16,20). In addition, it is possible that not all the reactivity observed in the TDL is GVHD-pathology related. For example, there may be some T cell responses to the flux in exposure to microbial agents due to early radiation induced intestinal epithelial damage. That notwithstanding, 75% of the $CD4^+$ Vβ families (Vβ2, 6, 7, 10, 11, and 13) and 66% of the $CD8^+$ Vβ families (Vβ8.2, 8.3, 14, and 16) that were found to be consistently skewed in the spleens of BALB.B recipient mice over a period of 40 days (10) were also skewed in at least two of the target tissues studied. Interestingly, the $CD4^+$V$\beta14^+$ family, which was also found to be skewed in BALB.B TDL, but was underrepresented in immunohistochemical analysis of lingual epithelium (8), was also not detected in the tissue spectratype analysis performed in the current study. This result suggests a lack of appropriate in situ target tissue expression of this particular miHA, and its expression may be limited to the hematopoietic/lymphoid compartment.

Our data supports the concept that some dominant miHA peptides in peripheral GVHD-target tissues can potentially drive a pattern of T cell alloreactivity different from that elicited in the hematopoietic/lymphoid compartment. In this regard, the $CD4^+$ T cell responses observed previously in the TDL were more congruent with the reactive skewings arising from specific tissue miHA, whereas $CD8^+$ T cells appeared to develop a more diverse response in the GVHD-target tissues. This result is consistent with the differences in the way in which class I and II-restricted Ags are presented, whereby $CD4^+$ T cells can encounter class II-restricted Ags presented on APC, regardless of location. In contrast, $CD8^+$ T cells tend to encounter the full breadth of their Ags at the tissue site where the Ags are derived.

Of particular interest are the $CD8^+$ V$\beta14^+$ and the $CD4^+$V$\beta2^+$ and $CD4^+$ V$\beta11^+$ T cell families, which were previously shown to have distinctive effects in the induction of lethal GVHD between the B6–>BALB.B and the B6–>CXB-2 strain combinations (7,9), and were also consistently skewed over time in transplanted BALB.B recipients (10). Host-presensitized $CD8^+$ V$\beta14^+$ T cells from B6 donors were expanded in all the GVHD-target tissues analyzed, with a single PCR-length: 152, commonly skewed (Table V). Sequence analysis of this CDR3-size peak revealed that this Vβ family exhibited preferential use of TCRJβ2.4 (10), suggesting

that the alloreactive expansion of the $CD8^+$ V$\beta14^+$ T cells was due to a unique miHA dominantly presented by GVHD-affected tissue. In addition, the BALB.B spectratype revealed two other skewed peaks not found in the CXB-2 recipients (7). Consistent with these results, in the present study, we observed that the BALB.B intestinal-infiltrating $CD8^+$ V$\beta14^+$ T cells had two distinct skewed peaks (158 and 161) (Table I), peaks not found in any tissue of the CXB-2 recipients. We also found that in the liver of CXB-2 mice, the peak at PCR-length 149 was uniquely skewed (Table I). In contrast to the $CD8^+$ V$\beta14^+$ family, $CD8^+$V$\beta4^+$ T cells showed a biased CDR3-size usage in BALB.B but not CXB-2 recipients (7). Spectratyping of tissue-infiltrating alloreactive T cells showed that this particular Vβ family was skewed in the spleens and livers of BALB.B mice (Table I; PCR-length peaks 187 and 190, respectively) and only in the livers of CXB-2 mice (Table I; PCR-length peaks 187 and 193). Taken together, the results suggest that differentially expressed miHA epitopes in both strains, as well as differential miHA expression across tissues, can determine the extent of T cell alloreactivity.

Both $CD4^+$Vβ2 and Vβ11 T cell families were reactive in the TDL, spleens, livers, and intestines of BALB.B mice (Table IV). Furthermore, sequence analysis of the TCR-CDR3 region of the Vβ11 family revealed a dominant oligoclonal response (10), demonstrating that the associated miHA responsible for eliciting the reactivity of this Vβ was ubiquitously and probably highly expressed across tissues, accounting for its dominant role in inducing severe lethal GVHD. Interestingly, although Vβ2 and Vβ11 were not skewed in the TDL of CXB-2 recipients, Vβ2 was skewed in all three tissues analyzed and Vβ11 was skewed in the livers and the spleens of these mice, but importantly not in the intestines (Table IV and Fig. 1), which contributes most to increased GVHD-related morbidity and mortality. In fact, B6 $CD4^+$V$\beta11^+$ T cells exhibited significant infiltration into BALB.B intestinal tissue, compared with that of CXB-2 recipients ($p \leq 0.01$). In addition, the number of apoptotic (TUNEL-positive) epithelial cells per tissue area was also significantly higher in BALB.B vs CXB-2 recipients ($p \leq 0.02$).

It should also be noted that the observation of alloreactive expansion, per se, does not always generate immunopathology of GVHD. As we have previously reported, the B6 $CD4^+$V$\beta5^+$ family, which was not skewed in the TDL of either BALB.B or CXB-2 mice, was reactive in the spleens, intestines and livers of BALB.B recipients and in the intestines and livers of CXB-2 recipients. However, previous work conducted in our laboratory demonstrated that infusion of purified B6 $CD4^+$V$\beta5^+$ T cells into lethally irradiated BALB.B recipients did not induce GVHD (9). Other factors can play a role in GVHD susceptibility, such as the increased expression of tenascin, an extracellular matrix protein involved in tissue regeneration and repair, and which has been shown to be protective against GVHD-mediated mucosal damage (21). Current work is being conducted in our laboratory to explore the possibility that higher expression of tenascin in the intestinal tissue of the CXB-2 mice may play a role in the inability of B6 $CD4^+$T cells to mediate lethal GVHD in this model.

In conclusion, results obtained in this study suggest that: 1) Differences in miHA presentation in GVHD-targeted tissues can affect the degree of severity of GVHD responses in MHC-matched miHA-disparate transplant situations; 2) T cell alloreactivity originating in the hematopoietic/lymphoid compartment can be lost in the target organ tissues, and in contrast, cryptic epitopes can be presented upon tissue damage, creating a distinct alloreactive pattern in the GVHD-target organs different from that found in the hematopoietic/lymphoid compartment; and 3) T cell alloresponses to miHA presented in more than one target organ and in some instances, in a particular tissue like the intestinal epithelium, can be associated with the severity of GVHD.

Acknowledgements

We thank Joshua Stern for technical assistance in performing some of the spectratype analyses.

References

1. Slavin S, Morecki S, Weiss L, Or R. Donor lymphocyte infusion: the use of alloreactive and tumor-reactive lymphocytes for immunotherapy of malignant and nonmalignant diseases in conjunction with allogeneic stem cell transplantation. J Hematother Stem Cell Res 2002;11:265–276. [PubMed: 11983098]
2. Nash RA, Storb R. Graft-versus-host effect after allogeneic hematopoietic stem cell transplantation: GVHD and GVL. Curr Opin Immunol 1996;8:674–680. [PubMed: 8902393]
3. Shlomchik WD. Graft-versus-host disease. Nat Rev Immunol 2007;7:340–352. [PubMed: 17438575]
4. Martin PJ, Hansen JA, Torok-Storb B, Moretti L, Press O, Storb R, Thomas ED, Weiden PL, Vitetta ES. Effects of treating marrow with a CD3-specific immunotoxin for prevention of acute graft-versus-host disease. Bone Marrow Transplant 1988;3:437–444. [PubMed: 2973360]
5. Patterson AE, Korngold R. Infusion of select leukemia-reactive TCR Vβ+ T cells provides graft-versus-leukemia responses with minimization of graft-versus-host disease following murine hematopoietic stem cell transplantation. Biol Blood Marrow Transplant 2001;7:187–196. [PubMed: 11349805]
6. Friedman TM, Azhipa O, Zilberberg J, Tkachuk Y, Hsu JW, Rowley SD, Goldberg SL, Korngold R, Pecora AL, Preti RA. Reconstitution of T cell subset repertoire diversity following multiple antigen-mismatched bone marrow transplantation. Biol Blood Marrow Transplant 2006;12:1092–1095. [PubMed: 17084373]
7. Friedman TM, Gilbert M, Briggs C, Korngold R. Repertoire analysis of $CD8^+$ T cell responses to minor histocompatibility antigens involved in graft-versus-host disease. J Immunol 1998;161:41–48. [PubMed: 9647205]
8. Friedman TM, Statton D, Jones SC, Berger MA, Murphy GF, Korngold R. Vβ spectratype analysis reveals heterogeneity of $CD4^+$ T-cell responses to minor histocompatibility antigens inved in graft-versus-host disease, correlations with epithelial tissue infiltrate. Biol Blood Marrow Transplant 2001;7:2–13. [PubMed: 11215694]
9. Jones SC, Friedman TM, Murphy GF, Korngold R. Specific donor Vβ-associated CD4 T-cell responses correlate with severe acute graft-versus-host disease directed to multiple minor histocompatibility antigens. Biol Blood Marrow Transplant 2004;10:91–105. [PubMed: 14750075]
10. Friedman TM, Jones SC, Statton D, Murphy GF, Korngold R. Evolution of responding $CD4^+$ and $CD8^+$ T-cell repertoires during the development of graft-versus-host disease directed to minor histocompatibility antigens. Biol Blood Marrow Transplant 2004;10:224–235. [PubMed: 15077221]
11. Berger MA, Korngold R. Immunodominant $CD4^+$ T cell receptor Vβ repertoires inved in graft-versus-host disease responses to minor histocompatibility antigens. J Immunol 1997;159:77–85. [PubMed: 9200441]
12. Berger M, Wettstein PJ, Korngold R. T cell subsets involved in lethal graft-versus-host disease directed to immunodominant minor histocompatibility antigens. Transplantation 1994;57:1095–1102. [PubMed: 7909395]
13. DiRienzo CG, Murphy GF, Friedman TM, Korngold R. T-cell receptor Vβ usage by effector $CD4^+ V\beta11^+$ T cells mediating graft-versus-host disease directed to minor histocompatibility antigens. Biol Blood Marrow Transplant 2007;13:265–276. [PubMed: 17317580]
14. Murphy GF, Sueki H, Teuscher C, Whitaker D, Korngold R. Role of mast cells in early epithelial target cell injury in experimental acute graft-versus-host disease. J Invest Dermatol 1994;102:451–461. [PubMed: 7908682]
15. Kusser KL, Randall TD. Simultaneous detection of EGFP and cell surface markers by fluorescence microscopy in lymphoid tissues. J Histochem Cytochem 2003;51:5–14. [PubMed: 12502749]
16. Griem P, Wallny HJ, Falk K, Rotzschke O, Arnold B, Schonrich G, Hammerling G, Rammensee HG. Uneven tissue distribution of minor histocompatibility proteins versus peptides is caused by MHC expression. Cell 1991;65:633–640. [PubMed: 2032287]

17. Rosset MB, Tieng V, Charron D, Toubert A. Differences in MHC-class I presented minor histocompatibility antigens extracted from normal and graft-versus-host disease GVHD mice. Clin Exp Immunol 2003;132:46–52. [PubMed: 12653835]

18. Korngold R, Wettstein PJ. Immunodominance in the graft-vs-host disease T cell response to minor histocompatibility antigens. J Immunol 1990;145:4079–4088. [PubMed: 2258608]

19. Gorski J, Yassai M, Zhu X, Kissela B, Kissella B, Keever C, Flomenberg N. Circulating T cell repertoire complexity in normal individuals and bone marrow recipients analyzed by CDR3 size spectratyping: correlation with immune status. J Immunol 1994;152:5109–5119. [PubMed: 8176227]

20. de Bueger M, Bakker A, Van Rood JJ, Van der Woude F, Goulmy E. Tissue distribution of human minor histocompatibility antigens: ubiquitous versus restricted tissue distribution indicates heterogeneity among human cytotoxic T lymphocyte-defined non-MHC antigens. J Immunol 1992;149:1788–1794. [PubMed: 1380540]

21. Stuber E, Von Freier A, Marinescu D, Folsch UR. Involvement of OX40-OX40L interactions in the intestinal manifestations of the murine acute graft-versus-host disease. Gastroenterology 1998;115:1205–1215. [PubMed: 9797376]

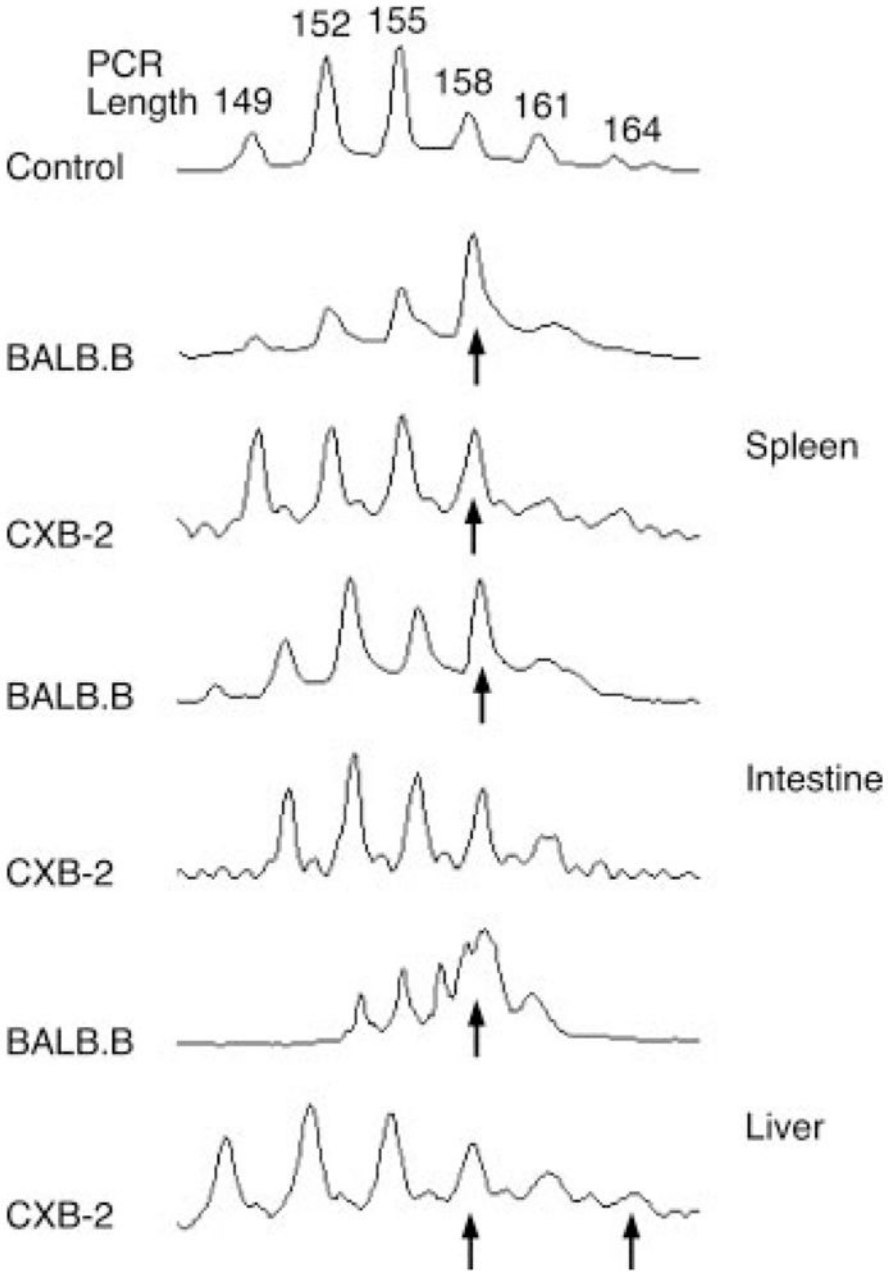

FIGURE 1.

Representative CDR3-size spectratype analysis of tissue-infiltrating B6 $CD4^+V\beta11^+$ T cells. BALB.B and CXB-2 mice were lethally irradiated and injected with 2×10^7 $CD8^+$ or $CD4^+$ enriched T cells from host-presensitized B6 mice. The liver, spleen, and the distal ileum were excised for further processing. The livers were dissociated by passage through a stainless steel mesh and the spleens were ground with a tissue grinder. Sections of the small intestine were flushed with PBS, cut into small pieces and processed to collect infiltrating lymphocytes before re-suspension in Ultraspec. Total cellular RNA, RT-PCR, and CDR3-size spectratype analysis was performed as previously described in the *Materials and Methods* section. A band was considered skewed if the mean area under the peak was greater than the mean ± 3× the SD of

the corresponding control peak (from naive B6 $CD4^+$ or $CD8^+$ T cells). Arrows indicate the presence of a skewed CDR3-size length.

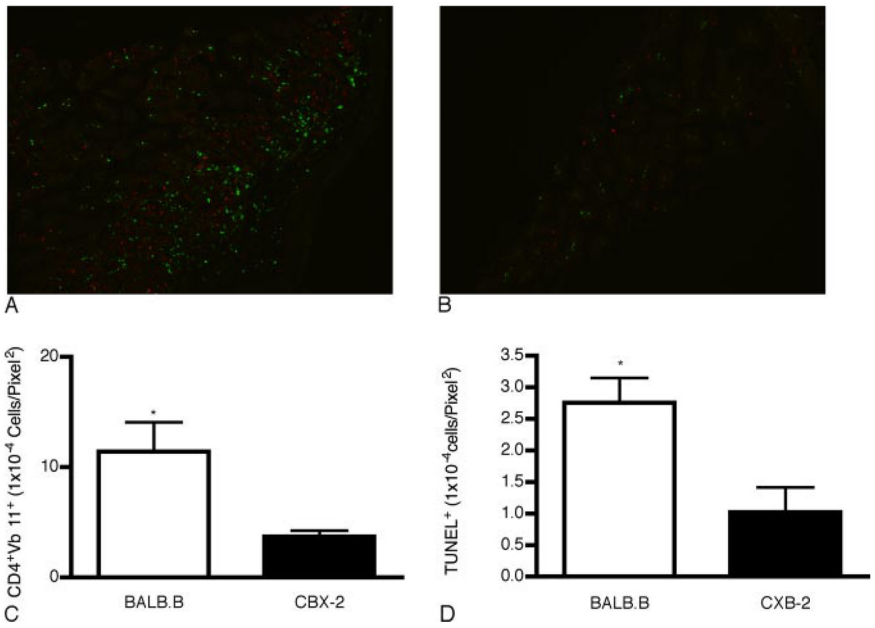

FIGURE 2.

GVHD-associated $CD4^+V\beta11^+$ infiltration and injury of intestinal epithelium. In brief, 4.6×10^5 $eGFP^+$ $CD4^+V\beta11^+$ cells were injected into lethally irradiated BALB.B and CXB-2 recipients. Greater numbers of $eGFP^+$ T cells (in green) and $TUNEL^+$ cells (in red) were observed in the intestine of BALB.B mice (*A*) compared with that of CXB-2 (*B*) recipients. *C*, Quantitative comparison of infiltrated $eGFP^+CD4^+V\beta11^+$ T cells per tissue area ($pixel^2$) ($p \leq 0.01$). *D*, TUNEL-positive cells per tissue area ($pixel^2$) ($p \leq 0.02$).

Table I

Comparison of the skewed CDR3-size lengths of host-presensitized B6 $CD8^+$ T cells from the GVHD-target organs of transplanted BALB.B versus CXB-2 recipient mice[a]

	Spleen		Intestine		Liver	
Vβ	**BALB.B**	**CXB-2**	**BALB.B**	**CXB-2**	**BALB.B**	**CXB-2**
1	—	192, 198	198, 201	192	—	192
2	—	167	—	152, 167	—	—
3	147, 150	153	147, 153	150	144	—
4	187	—	—	—	190	187, 193
5	—	—	185	—	—	—
6	—	155	—	—	**149**	**149**, 155
7	**180**	**180**, 186	**180**	**180**, 186	180, **186**	**186**
8.1	139	148	**136**, 139	**136**	142	—
8.2	**151**	**151**	—	151	151	145
8.3	156, 162	—	153, 162	156	156	168
9	—	—	147	—	153	—
10	138	—	**147**	144, **147**	132, 144	—
11	—	157	154	157	—	157
12	—	—	—	201	—	204
13	—	—	172	—	—	160
14	**152**, **164**	**152**, **164**	**152**, 158,* 161*	**152**, 164	**152**	149, **152**, 164
15	183	—	**183**	**183**	177	183
16	145	—	145	154	145	154
18	**222**	**222**	**207**	**207**, 222	207	207
20	197, **200, 203**	188, **200, 203**	200, 203	194	197, 200	191, 203

[a]Lethally irradiated BALB.B and CXB-2 mice were injected with 2×10^7 host-presensitized B6 donor T cells, respectively. GVHD-target tissue infiltrating lymphocytes were isolated and CDR3-size spectratype analysis was performed as described in the *Materials and Methods* section. CDR3-size length skewing was determined by comparison of the experimental spectratypes to those of normal B6 control for the respective Vβ family; the highlighted bands are common to both BALB.B and CXB-2 recipients; —, No skewing; ND, Not determined;

*, Unique skewing. Results were averaged from three separate experiments.

Table II

Comparison of the skewed CDR3-size lengths of host-presensitized B6 $CD4^+$ T cells from the GVHD-target organs of transplanted BALB.B versus CXB-2 recipient mice[a]

	Spleen		Intestine		Liver	
Vβ	BALB.B	CXB-2	BALB.B	CXB-2	BALB.B	CXB-2
1	—	—	—	—	183	—
2	**167**	**167**	**167**	**167**	**167**	158, **167**
3	—	148	—	ND	—	—
4	—	—	—	—	—	—
5	176	—	**176**	**176**	**176**	**176**
6	ND	143	141,143	—	143	153
7	—	180	171	180	171,177,186	180
8.1	ND	—	ND	—	ND	ND
8.2	ND	—	ND	136	136,139	ND
8.3	172	157	172	154,157	172	160
9	**153**,156	**153**	**153**,156	142,**153**	**153**	142,**153**,156
10	**130**,132	**130**	**130**,132,136	**130**	**130**,132	**130**
11	**158**	**158**	**158**	—	**158**	**158**, 164
12	—	—	—	—	—	208
13	**160**,163,178	**160**	ND	160	163	160
14	ND	158	ND	ND	ND	ND
15	—	—	ND	—	165,168	—
16	ND	157	ND	ND	ND	—
18	ND	219	ND	219	ND	216
20	—	197	ND	194, 197	185, 189, 203	197

[a] CDR3-size lengths skewed compared to that of normal B6 control mice for the respective Vβ family; the highlighted bands are common to both BALB.B and CXB-2 recipients; —, No skewing; ND, Not determined;

*, Unique skewing.

Table III

Comparison of the skewed CDR3-size lengths of reactive B6 CD8$^+$ T cells in TDL to the tissue-infiltrating B6 T cells in BALB.B and CXB-2 recipients

	BALB.B CD8+ T cells				CXB-2 CD8+ T cells			
Vβ	TDL (7)	Spleen	Intestine	Liver	TDL (7)	Spleen	Intestine	Liver
1	+	—	+	—	+	+	+	+
2	—	—	—	—	—	+	+	—
3	—	+	+	+	—	+	+	—
4	+	+	—	+	—	—	—	+
5	—	—	+	—	—	—	—	—
6	+	—	—	+	+	+	—	+
7	—	+	+	+	—	+	+	+
8.1/.2/.3*	+	+	+	+	+	+	+	+
9	+	—	+	+	+	—	—	—
10	+	+	+	+	+	—	+	—
11	+	—	+	—	+	+	+	+
12	—	—	—	—	—	—	+	+
13	—	—	+	—	—	—	—	+
14	+	+	+	+	+	+	+	+
15	—	+	+	+	—	—	+	+
16	—	+	+	+	—	—	+	+
20	—	+	+	+	—	+	+	+

+, At least one CDR3-size lengths was significantly skewed compared to that of normal B6 control for the respective Vβ family. —, No skewing, ND, No data.

*, Vβ 8.1, 8.2 and 8.3 combined in order to compare to previous data.

Table IV

Comparison of the skewed CDR3-size lengths of reactive B6 CD4$^+$ T cells in TDL to the tissue-infiltrating B6 T cells in BALB.B and CXB-2 recipients

	BALB.B CD4+ T cells				CXB-2 CD4+ T cells			
Vβ	TDL (8)	Spleen	Intestine	Liver	TDL (8)	Spleen	Intestine	Liver
1	—	—	—	+	—	—	—	—
2	+	+	+	+	—	+	+	+
3	—	—	—	—	—	+	ND	—
4	+	—	—	—	+	—	—	—
5	—	+	+	+	—	—	+	+
6	+	ND	+	+	+	+	—	+
7	+	—	+	+	+	+	+	+
8.1/.2/.3*	+	+	+	+	+	+	+	+
9	+	+	+	+	+	+	+	+
10	+	+	+	+	+	+	+	+
11	+	+	+	+	—	+	—	+
12	+	—	—	—	+	—	—	+
13	+	+	ND	+	+	+	+	+
14	+	ND	ND	ND	+	+	ND	ND
15	—	—	ND	+	—	—	—	—
16	—	ND	ND	ND	+	+	ND	—
18	ND	ND	ND	ND	+	+	+	+
20	—	—	ND	+	—	+	+	+

+, At least one CDR3-size length was significantly skewed compared to that of normal B6 control for the respective Vβ family. —, No skewing; ND, No data;

*, Vβ 8.1, 8.2, and 8.3 combined in order to compare to previous data.

Table V

Overlapping Vβ skewing of presensitized B6 CD8$^+$ T cells between tissues in BALB.B and CXB-2 recipient mice[a]

	BALB.B		CXB-2	
Vβ	**Length**	**Tissue**	**Length**	**Tissue**
1			192	S, I, L
2			167	S, I
3	147	S, I		
4				
5				
6			155	S, L
7	180	S, I, L	180,186	S, I, L
8.1	139	S, I, L		
8.2	151	S, L	151	S, I
8.3	162; 156	S, I; L, S		
9				
10				
11			157	S, I, L
12				
13				
14	152	S, I, L	152,164	S, I, L
15	183	S, I	183	I, L
16	145	S, I, L	154	I, L
18	207	S, L	207; 222	I, L; S, I
20	200; 197; 203	S, I, L; S, L; S, I	203	S, L

[a]CDR3-size lengths significantly skewed compared to that of normal B6 control for the respective Vβ family. S, Spleen; I, Intestine; and L, Liver.

Table VI

Overlapping Vβ skewing of presensitized B6 CD4$^+$ T cells between tissues in BALB.B and CXB-2 recipient mice[a]

	BALB.B		CXB-2	
Vβ	Length	Tissue	Length	Tissue
1				
2	167	S, I, L	167	S, I, L
3				
4				
5	176	S, I, L	176	I, L
6	143	I, L		
7	171; 176	I, L; S, L	180	S, I, L
8.1				
8.2				
8.3	173	S, I, L	157	S, I
9	153; 156	S, I, L; S, I	153; 142	S, I, L; I, L
10	130,132	S, I, L	130	S, I, L
11	158	S, I, L	158	S, L
12				
13	163	S, L	160	S, I, L
14				
15				
16				
18			219	S, I
20			197	S, I, L

[a]CDR3-size lengths significantly skewed compared to that of normal B6 control for the respective Vβ family. S, Spleen; I, Intestine; and L, Liver.